Chinese Journal of
POLYMER SCIENCE

RESEARCH ARTICLE

https://doi.org/10.1007/s10118-024-3128-2
Chinese J. Polym. Sci. **2024**, *42*, 976–983

A Radiative-Cooling Hierarchical Aligned Porous Poly(vinylidene fluoride) Film by Freeze-Thaw-Promoted Nonsolvent-Induced Phase Separation

Yiting Zhang[a], Jiahui Sun[a], Yufeng Wang[b], Yunchen Wu[a], Chun Huang[a], Chao Zhang[b*], and Tianxi Liu[a*]

[a] *Key Laboratory of Synthetic and Biological Colloids Ministry of Education, School of Chemical and Material Engineering, Jiangnan University, Wuxi 214122, China*
[b] *State Key Laboratory for Modification of Chemical Fibers and Polymer Materials, College of Materials Science and Engineering, Donghua University, Shanghai 201620, China*

Electronic Supplementary Information

Abstract Passive daytime radiative cooling (PDRC) is an innovative and sustainable cooling technology that holds immense potential for addressing the energy crisis. Despite the numerous reports on radiative coolers, the design of a straightforward, efficient, and readily producible system remains a challenge. Herein, we present the development of a hierarchical aligned porous poly(vinylidene fluoride) (HAP-PVDF) film through a freeze-thaw-promoted nonsolvent-induced phase separation strategy. This film features oriented microporous arrays in conjunction with random nanopores, enabling efficient radiative cooling performance under direct sunlight conditions. The incorporation of both micro- and nano-pores in the HAP-PVDF film results in a remarkable solar reflectance of 97% and a sufficiently high infrared thermal emissivity of 96%, facilitating sub-environmental cooling at 18.3 °C on sunny days and 13.1 °C on cloudy days. Additionally, the HAP-PVDF film also exhibits exceptional flexibility and hydrophobicity. Theoretical calculations further confirm a radiative cooling power of 94.8 $W \cdot m^{-2}$ under a solar intensity of 1000 $W \cdot m^{-2}$, demonstrating a performance comparable to the majority of reported radiative coolers.

Keywords Daytime radiative cooling; Hierarchical porosity; PVDF porous film; Thermal insulation; Nonsolvent-induced phase separation

Citation: Zhang, Y.; Sun, J.; Wang, Y.; Wu, Y.; Huang, C.; Zhang, C.; Liu, T. X. A radiative-cooling hierarchical aligned porous poly(vinylidene fluoride) film by freeze-thaw-promoted nonsolvent-induced phase separation. *Chinese J. Polym. Sci.* **2024**, *42*, 976–983.

INTRODUCTION

The current global energy crisis and escalating environmental concerns have intensified the demand for novel thermal management materials and technologies with low to zero carbon emissions, aiming to overcome the existing impasse.[1,2] A promising solution is the emerging passive daytime radiative cooling (PDRC) technology, which enables passive cooling of surface objects without any energy consumption.[3–5] PDRC technology operates by reflecting sunlight to minimize external energy absorption while radiating heat into the cold reaches of the universe through electromagnetic waves within the range of 8–13 μm, able to penetrate the atmosphere.[6–8] In recent years, various radiative cooling materials have been developed to achieve high solar reflectance by manipulating the interaction between sunlight and matter on a subwavelength scale. Based on their structural design and composition, radiative coolers can be classified into four groups.[9,10] Photonic multilayer structures employ nanometer-thick dielectric layers in combination with reflective silver layers to efficiently reflect sunlight.[11,12] Metamaterials achieve effective sunlight reflection primarily through templated three-dimensional structured polymers.[13,14] Particle composite structures introduce nanoparticles into polymers to achieve high emissivity and reflectivity through phonon polarization resonance.[15,16] Porous structures enhance sunlight reflection and scattering by controlling pore size, making them a crucial research focus for daytime radiative cooling materials due to their simplicity, cost-effectiveness, and high performance.[17–19]

Recent studies demonstrated that replacing the reflective metal layer with a porous light-scattering cavity significantly enhances the modulation of optical performance to an advanced level.[20,21] The underlying mechanism of porous structures relies on Mie scattering, which is most effective when the aperture diameter closely matches the wavelength of the target light.[22] The mean free path of photons generated by micrometer-sized pores corresponds to the wavelength of near-infrared light, enabling efficient sunlight scattering.[20] Pores with characteristic sizes in the range of tens or hundreds of nanometers strongly scatter shorter visible wave-

* Corresponding authors, E-mail: czhang@dhu.edu.cn (C.Z.)
E-mail: txliu@jiangnan.edu.cn (T.X.L.)

Special Issue: Functional Polymer Materials
Received January 30, 2024; Accepted March 20, 2024; Published online May 7, 2024

lengths.[23] Consequently, radiative coolers with porous structures necessitate the construction of multi-level pore structures and pore size distributions to scatter sunlight across different wavelengths. However, the development of such multi-level pore structure porous materials still faces significant challenges at present.

Here, we present the fabrication of a hierarchical aligned porous poly(vinylidene fluoride) (HAP-PVDF) film using a freeze-thaw-promoted nonsolvent-induced phase separation approach. This film fulfills the requirements of porous radiative coolers at both the molecular level and the nano/micron scale, enabling efficient radiative cooling under direct sunlight. The micro-nano structure of the film ensures a substantial solar reflectance of 97% and infrared thermal emissivity of 96%. Additionally, the directional pores within the film impede thermal conduction in the direction perpendicular to the skeleton wall, resulting in a low thermal conductivity in that direction and minimizing ambient heat gain. Under exposure to a humid subtropical climate and a solar intensity of 900 $W \cdot m^{-2}$, the HAP-PVDF film exhibited a remarkable sub-ambient temperature reduction of more than 18.3 °C. Furthermore, the HAP-PVDF films displayed high contact angles and excellent flexibility, rendering them highly appealing for self-cleaning applications in building environments. This study is expected to provide novel insights into the preparation of hierarchical porous structures and their diverse applications across various fields.

EXPERIMENTAL

Materials

Dimethyl sulfoxide (DMSO, AR, ≥99.5%) and poly(vinyl pyrrolidone) (PVP, K30) were purchased from Sinopharm Chemicals. Poly(vinylidene fluoride) (PVDF) powder (average M_w=2.75×10^5) was purchased from Aladdin Reagents. Deionized water was produced through Direct-Q (France) and used throughout the experiments.

Preparation of HAP-PVDF Films

PVDF (10 g) and PVP (1 g) were homogeneously dissolved into 50 g of DMSO under 60 °C. Subsequently, the solution was poured into a polytetrafluoroethylene mold with a copper base. To achieve directional freezing, the bottom copper was brought into contact with liquid nitrogen. After freezing, the film was immersed in water for 24 h to induce freeze-thaw-promoted nonsolvent-induced phase separation, with the water being changed every 12 h to ensure thorough removal of PVP and DMSO. The resulting film was then dried at 30 °C for 12 h, for producing the HAP-PVDF film. For comparison, an aligned porous PVDF (AP-PVDF) film was prepared by directly freeze-drying the directionally frozen precursor film. Additionally, an hierarchical porous PVDF (HP-PVDF) film was prepared from the precursor solution using the conventional nonsolvent-induced phase separation method, where the precursor solution was cast onto a polytetrafluoroethylene substrate, immersed in water for 36 h, and dried at 30 °C for 12 h.

Characterization

SEM observation was conducted using a Hitachi S-4800 field-emission scanning electron microscope at an accelerating voltage of 3 kV. FTIR spectra were obtained using a Thermofisher Nicolet 6700 attenuation reflectance FTIR spectrometer. Solar reflectance of film samples was measured using a UV-Vis-NIR spectrophotometer Lambda 750 equipped with a polytetrafluoroethylene integrating sphere. Reflectance and transmittance in the mid-infrared wavelength ranges were determined using an FTIR spectrometer Nicolet IS50 with a gold integrating sphere. Thermal conductivity measurements were performed using a Hot Disk TPS 2500S apparatus. Mechanical properties were assessed using a Suns Technology universal UTM2203 tensile testing machine. Infrared pictures were captured using a portable thermal imaging camera (Fluke, Ti400+).

RESULTS AND DISCUSSION

The disparate solubility of PVDF and PVP in various solvents is a fundamental requirement for creating hierarchical porous structures. PVDF dissolves readily in highly polar organic solvents such as DMF, NMP, acetone, and DMSO, but remains insoluble in water. Conversely, PVP exhibits high solubility in both water and most organic solvents. Based on Table S1 (in the electronic supplementary information, ESI), DMSO, which possesses the highest melting point of 18 °C, was selected as the solvent. The preparation of layered porous HAP-PVDF films involved a two-step process of directional freezing and phase separation, as illustrated in Fig. 1(a). Initially, a uniform coating of a PVDF and PVP mixture in DMSO was applied to the substrate using a scraper. Subsequently, the solution was subjected to low-temperature unidirectional freezing, causing DMSO to crystallize and form an oriented crystal structure. This enabled the concentration enrichment of PVDF and PVP within the oriented crystal structures, leading to the formation of a precursor material with oriented microchannels. The frozen precursor sample was then immersed in deionized water to facilitate solvent and non-solvent substitution. During the solvent substitution process, three simultaneous processes occurred: (1) PVDF replicated the DMSO, orienting the ice crystal template and establishing an oriented structural backbone. Since water is a non-solvent for PVDF, this step proceeded rapidly;[24,25] (2) PVP rapidly dissolved in water, resulting in the formation of nanoscale pores within the PVDF-based pore wall structure. The proportion of PVP in PVDF was carefully controlled to prevent channel collapse; and (3) the DMSO templates were gradually replaced by water, leading to the formation of oriented pore channel structures. The cured molded PVDF exhibited excellent structural stability, and water was removed using conventional oven drying methods.[24] For comparative purposes, PVDF films were also prepared using conventional techniques such as the directed freeze-freeze-drying method (referred to as aligned porous PVDF films, AP-PVDF) and the conventional non-solvent induced phase separation method (referred to as hierarchical porous PVDF films, HP-PVDF).

The HAP-PVDF films exhibited several notable characteristics: they were opaque, white, mechanically robust, and had a large area. As depicted in Fig. 1(b), these films can be precisely trimmed and normalized into various shapes, such as circles, triangles, and rectangles. Remarkably, even after undergoing full twisting induced by torsional force, the film remains intact and fully restores to its original shape (Fig. 1c). These unique attributes hold significant potential for diverse applications in architecture. Furthermore, the HAP-PVDF films

https://doi.org/10.1007/s10118-024-3128-2

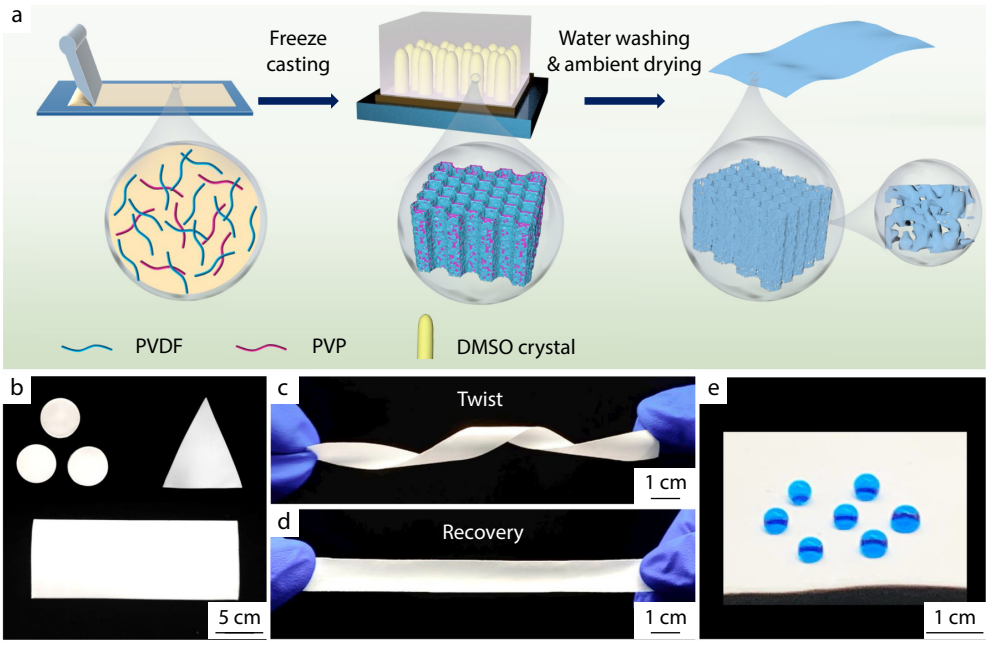

Fig. 1 Fabrication and characterization of HAP-PVDF films. (a) Schematic illustration of the fabrication of HAP-PVDF films; (b) Photograph of HAP-PVDF films cut into various shapes; Photographs of HAP-PVDF films (c) deformed by torsional force and (d) recovered to original shapes; (e) Photograph demonstrating the hydrophobicity of HAP-PVDF film.

display hydrophobic properties, rendering them impervious to water and exhibiting excellent self-cleaning capabilities (Fig. 1d). In comparison to the HP-PVDF film, the contact angle of the HAP-PVDF film demonstrates hydrophobic properties and remains essentially constant (Fig. 1e). In contrast, the AP-PVDF films absorbed small amounts of water due to the presence of residual PVP (Fig. S1 in ESI). These results indirectly confirmed the effective removal of PVP from the HAP-PVDF and HP-PVDF films during the phase separation process.

Scanning electron microscopy (SEM) observations were employed to investigate the surface and internal structure of various PVDF films. Both the HAP-PVDF and AP-PVDF films exhibited aligned channels when observed from the surface (Figs. 2a and 2d). However, a notable distinction can be observed in the bottom pore walls: the HAP-PVDF films displayed significantly thicker walls compared to the AP-PVDF films, along with randomly distributed disordered nanoscale pores (Figs. 2b and 2f). The formation of pore morphology is primarily influenced by the dissolution of PVP in water. During the phase separation process, the film surface came into direct contact with deionized water, leading to the dissolution of PVP and subsequent diffusion of PVDF and resulting in the thickening of the bottom pore walls.[26,27] The HAP-PVDF films exhibit a porous structure with micropores ranging from 2 μm to 5 μm, accompanied by secondary nanostructures comprising nanopores ranging from 50 nm to 500 nm (Fig. S2 in ESI). SEM image of the HAP-PVDF film without added PVP presented in Fig. S3 (in ESI) reveals well-aligned channels and smooth pore walls with no visible nanopores on the surface. Notably, the bottom part of the film maintains a thin wall thickness. This observation confirms that the nanopores in the HAP-PVDF films result from the subsequent dissolution of added PVP. Increasing the PVP content in the films causes the gradual collapse of longitudinally aligned channels, resulting in only a small number of nanopores on the surface, while the micropores become completely blocked. This collapse occurs due to the significant increase in pore diameter and number within the pore walls caused by the high PVP content, which triggers the collapse of the aligned channels. Besides, the AP-PVDF films solely display micropores ranging from 1 μm to 5 μm (Fig. S4 in ESI). The HAP-PVDF films also show a distinctive porous topological structure, characterized by interconnected micropores similar to the AP-PVDF films (Figs. 2c and 2f). The side pore walls of the HAP-PVDF films also exhibit randomly distributed disordered nanoscale pores, although without significant thickening. This observation suggests that the diffusion of PVDF may be impeded by the presence of solidified DMSO. As for the HP-PVDF films, both the surface and interior display an identical structure comprising randomly distributed nanopores in the size range of 50–600 nm, devoid of any micrometer-sized pore structures, as depicted in Figs. 2(g)–2(i) and Fig. S5 (in ESI).

The PVDF films underwent FTIR spectroscopy analysis to investigate their bonding and absorbance wavelengths. The molecular vibrations of C—F and C—H at 876, 1170 and 1405 cm^{-1} were attributed to PVDF and fell within the atmospheric window (Fig. 3a), resulting in strong infrared absorption/emission. The vibrational band of C=O at 1648 cm^{-1} is absent in the HAP-PVDF and HP-PVDF films, unlike in the AP-PVDF films. This observation suggests that PVP was completely removed during the phase separation process, consistent with previous literature.[28] The presence of PVP not only leads to moisture absorption but also reduces the thermal stability of the film (Fig. S6 in ESI). In practical applications, the mechanical strength of radiative cooling materials is a crucial factor that must withstand external forces. Our films exhibit remarkable flexibility and mechanical strength (Fig. 3b), owing to the tightly arranged PVDF molecular chains. Notably,

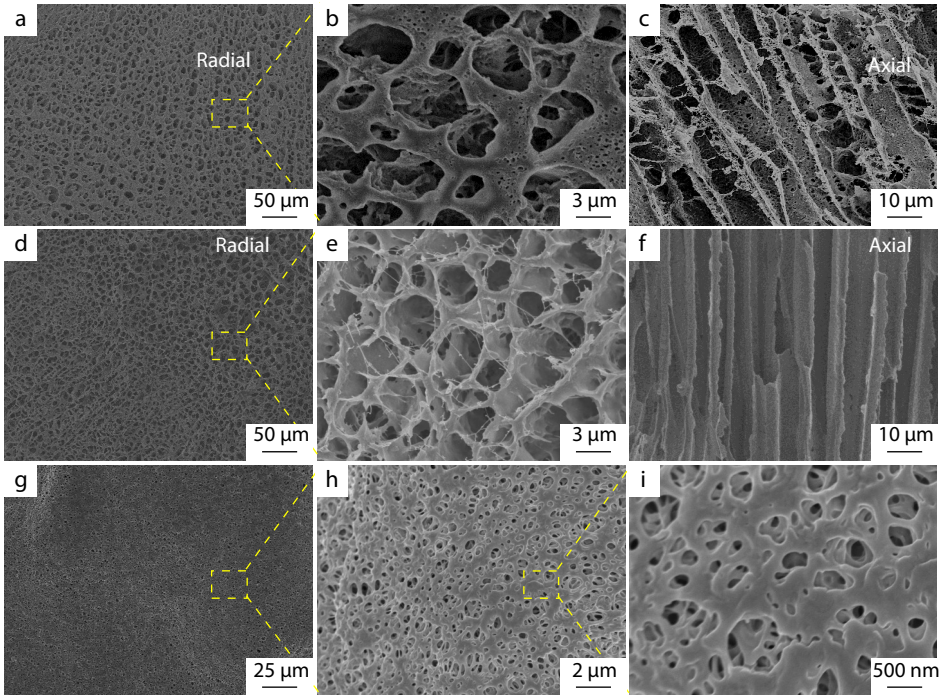

Fig. 2 Morphologies of HAP-PVDF, AP-PVDF and HP-PVDF films. (a, b) Top and (c) side view of HAP-PVDF film; (d, e) Top and (f) side view of AP-PVDF film; (g–i) Top view of HP-PVDF film.

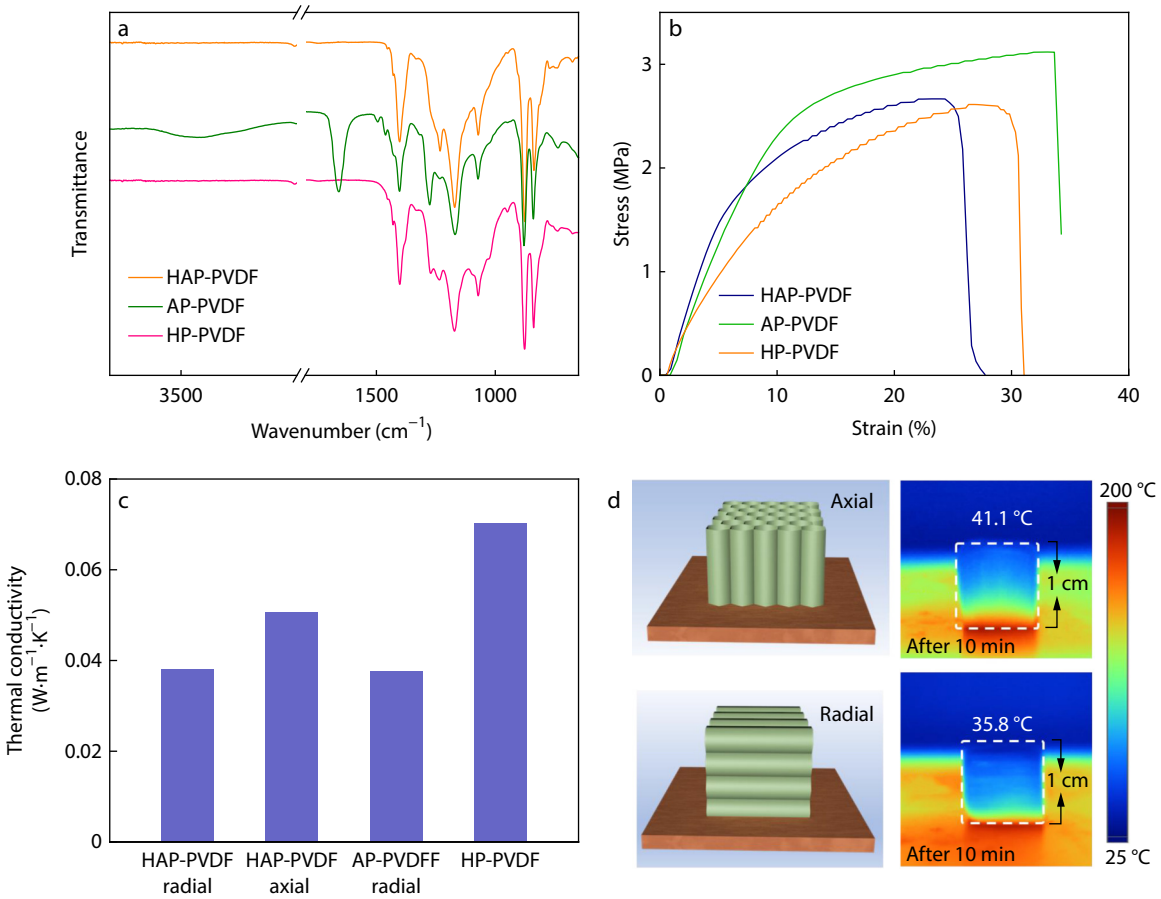

Fig. 3 Characterization of HAP-PVDF films: (a) FTIR spectra, (b) stress-strain curves, and (c) thermal conductivities of HAP-PVDF, AP-PVDF and HP-PVDF films; (d) Thermal insulation properties of HAP-PVDF film in axial and radial directions.

https://doi.org/10.1007/s10118-024-3128-2

the tensile strength of the AP-PVDF films (3 MPa) surpasses that of the HAP-PVDF and HP-PVDF films (2.5 MPa), which is attributed to the small amount of PVP with the plasticizing effect enhancing the ductility of the film.[29] Effective thermal insulation is crucial for countering dynamic temperature changes and enhancing cooling efficiency. As depicted in Fig. 3(c), the thermal conductivities of the HAP-PVDF and AP-PVDF films in the radial direction are similar to each other at 0.038 $W·m^{-1}·K^{-1}$. In contrast, the thermal conductivities of the HP-PVDF and HAP-PVDF films in the axial direction are 0.070 and 0.050 $W·m^{-1}·K^{-1}$, respectively, both are higher than that of the HAP-PVDF film in the radial direction. This disparity arises because air has a relatively lower thermal conductivity compared to solids, resulting in poorer heat transfer in the axial direction. The thermal infrared plots further confirm that radial heat penetration in the HAP-PVDF film occurs at a slower rate than axial heat transfer (Fig. 3d).

The optical properties of PVDF films in both the visible and infrared regions were quantitatively characterized. Through the morphology design strategy, the HAP-PVDF films exhibit a significantly higher solar irradiation reflectance of 97% (0.3–2.5 μm), which is comparable to other radiative cooling materials in previous literatures,[6,16,18,21,30,32] and surpassing that of the AP-PVDF (90%) and HP-PVDF (78%) films (Fig. 4a). This enhancement is attributed to the sunlight scattering effect resulting from the widely distributed oriented micrometer and nanopores. The microporous structures of HAP-PVDF films, ranging in size from approximately 2 μm to 5 μm, effectively scatters sunlight. This scattering effect is further enhanced by the scattering of shorter wavelengths of visible light through nanopores sized around 50 nm to 500 nm. The HAP-PVDF film exhibits high reflectance across the entire solar spectrum, spanning from 0.3 μm to 2.5 μm. In contrast, the HP-PVDF film displays a sudden increase in reflectance within the shorter visible range, attributed to the enrichment of its nanopores, while the AP-PVDF film, lacking a nanoporous structure, shows significantly lower reflectivity compared to the HAP-PVDF film. Within the atmospheric transparency window (8–13 μm), the emissivities of the three PVDF film types remain relatively consistent, reaching up to 96% (Fig. 4b). This variation primarily stems from the chemical vibrations of C—F and C—H. Figs. 4(c) and 4(d) present the emissivity spectra of the HAP-PVDF films at different polarization angles. Remarkably, the emissivity within the atmospheric window remained nearly constant over a wide range of polarization angles, ranging from 10° to 80°, with an average emissivity exceeding 95%. These findings demonstrate that the HAP-PVDF film not only exhibits excellent reflectance, eliminating the need for a silver reflector employed in previous designs but also effectively radiates energy into the universe through the atmospheric window. By measuring the reflectance and emissivity of the material, the net cooling power during both day and night can be calculated using the radiative cooling theory model, as depicted in Fig. 4(e) and Fig. S7 (in ESI). Assum-

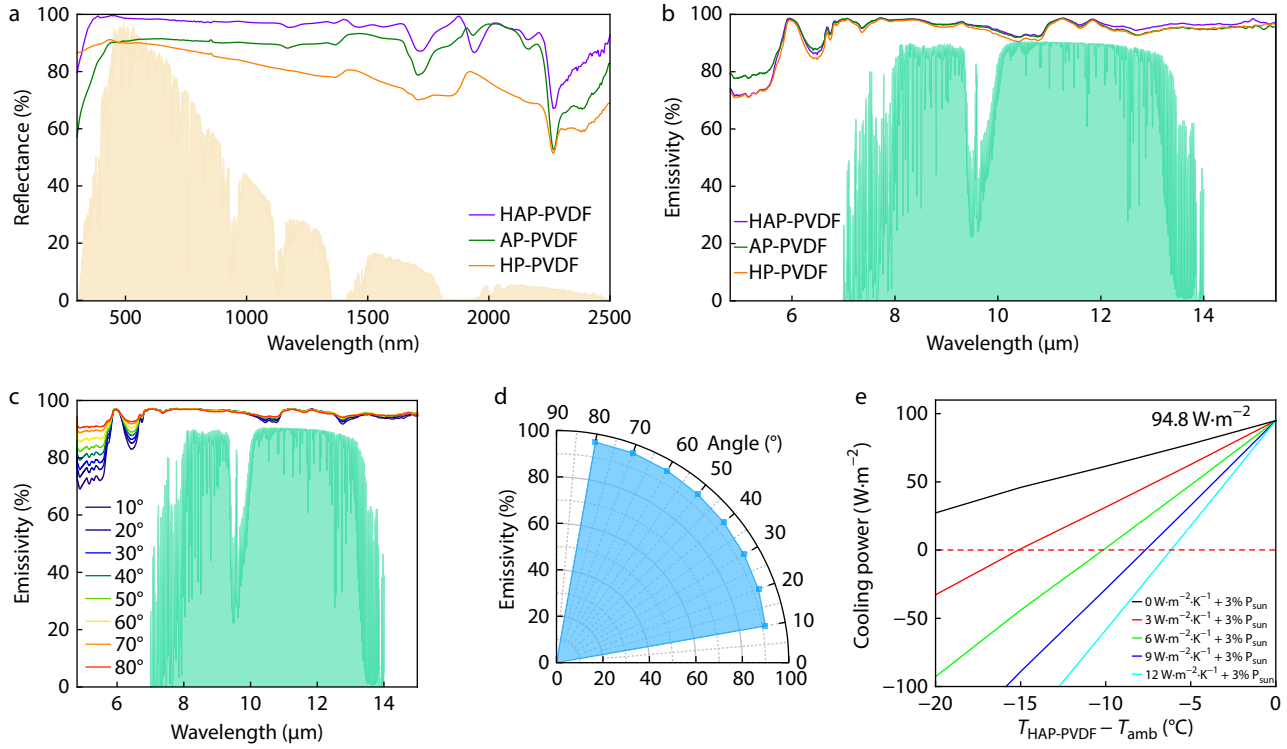

Fig. 4 Spectroscopy and cooling power of HAP-PVDF films. (a) UV-Vis-IR reflectance (yellow shaded area of standardized ASTM G173 global solar spectrum), and (b) infrared emissivity spectra of HAP-PVDF, AP-PVDF and HP-PVDF films; (c) Infrared emissivity spectra of HAP-PVDF film at different angles (θ) from 10° to 80°. Green shaded areas in (b, c) are the atmospheric transparency window; (d) Average emissivity of HAP-PVDF film against atmospheric transparent window at angles from 10° to 80°; (e) Calculated cooling power of HAP-PVDF film at a fixed ambient temperature and solar intensity of 30 °C and 1000 $W·m^{-2}$, respectively. Here, 0, 3, 6, 9 and 12 $W·m^{-2}·K^{-1}$ are set for non-radiative heat transfer coefficients.

https://doi.org/10.1007/s10118-024-3128-2

ing an ambient temperature (T_{amb}) of 32 °C (constant throughout day and night time) and a solar radiation power of 1000 W·m^{-2} for simplification purposes, the maximum cooling power during nighttime and daytime operations reaches 124.8 and 94.8 W·m^{-2}, respectively.

The sub-ambient PDRC performance of PVDF films is significantly influenced by various weather conditions, including solar irradiation, cloud cover, ambient humidity, ambient temperature, and wind speed.[30–32] Here, we conducted tests to evaluate the effect of climate on the radiative cooling of PVDF films (Fig. S8 in ESI). The test site, Wuxi City in China, experiences a subtropical monsoon climate with variable weather patterns, providing diverse conditions for our measurements. As illustrated in Figs. 5(a)–5(c), under clear and cloudless weather conditions with a consistent humidity level of approximately 42% throughout the day, all three types of PVDF films exhibit maximum sub-ambient cooling at noon, with the HAP-PVDF film demonstrating the most significant temperature decrease of 18.3 °C. Even at around 2:00 p.m., when the solar intensity dropped considerably at the test site due to the obstruction of sunlight by surrounding buildings (from 700 W·m^{-2} to 125 W·m^{-2}), the PVDF films still managed to lower the ambient temperature by approximately 5.9, 4.8 and 3.1 °C, respectively. The test results under cloudy weather conditions indicated that the cooling effect of all three types of PVDF films was affected, exhibiting fluctuations in cooling performance due to reduced solar irradiation and increased humidity (Figs. 5d–5e). Nevertheless, the HAP-PVDF film achieved a remarkable maximum sub-ambient cooling of 13.1 °C, with an average cooling reduction of 7 °C (Fig. 5f). By comparing the results of these two tests, we can conclude that weather conditions indeed impact the PDRC performance of PVDF films, consistent with previous findings in the literature.[33]

The practical feasibility of using PVDF films as scalable PDRC materials was verified through scenario-based experiments. Four identical house models were covered with HAP-PVDF, AP-PVDF, HP-PVDF, and uncovered (blank), and temperature changes were monitored for 60 min under direct sunlight (Fig. 5g). Upon reaching a thermal steady state, thermal infrared imaging revealed significant temperature variations among the four roofs, measuring 31.6, 30.4, 28.3 and 35.6 °C, respectively, with the HAP-PVDF film demonstrating the most effective temperature reduction (Fig. 5h). Thermocouple measurements also consistently indicated that the roof covered by the HAP-PVDF film maintained lower temperatures compared to the other three roofs, rather than being specific to a particular moment in time (Fig. 5i). To ensure repeatability, the same test was conducted on radiative cooling films under cloudy weather conditions. Throughout the 30-

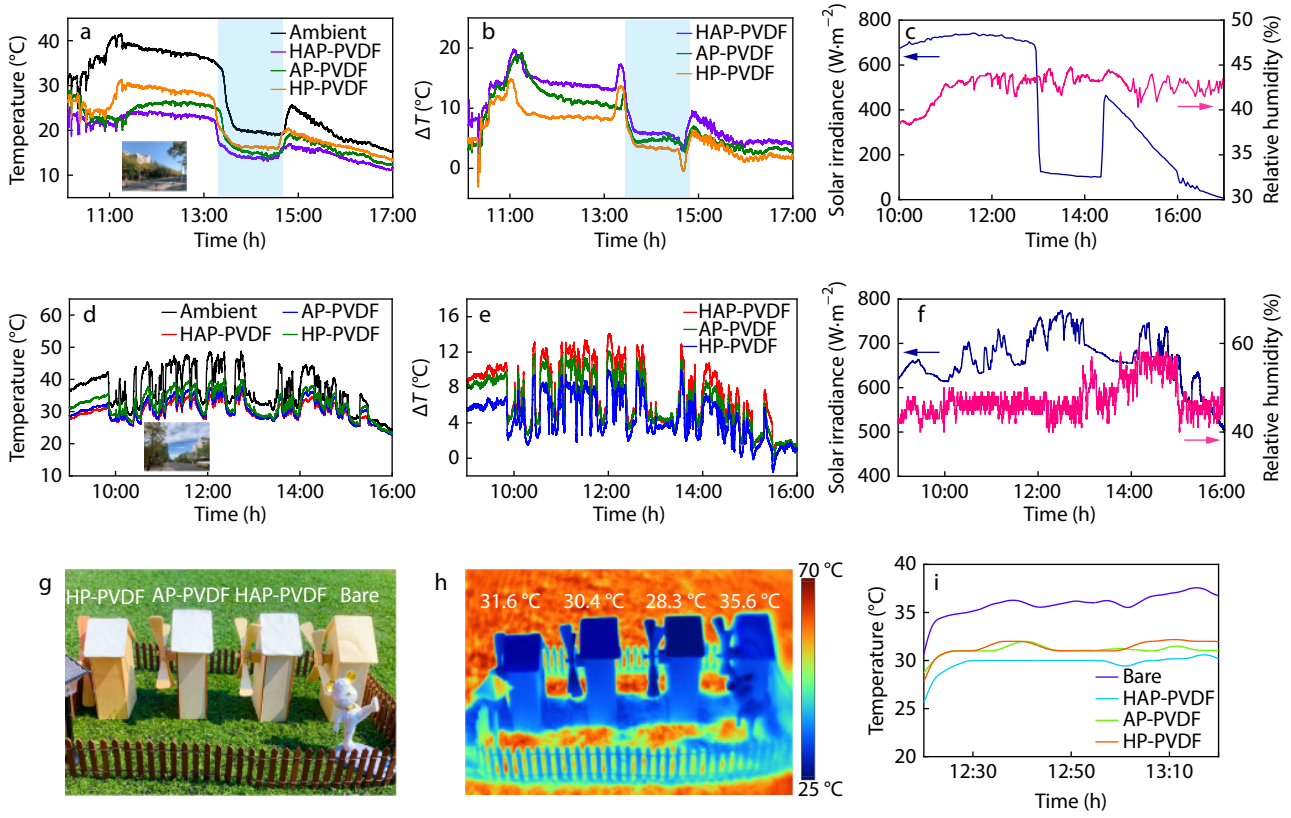

Fig. 5 Daytime radiative cooling performance of HAP-PVDF films in various weather conditions. (a) Real-time temperatures of outdoor radiative cooling experiments with HAP-PVDF, AP-PVDF and HP-PVDF films on a sunny day; (b) Corresponding sub-ambient temperature drops (ΔT); (c) Solar irradiance and ambient relative humidity; (d) Real-time temperatures of outdoor experiments with HAP-PVDF, AP-PVDF and HP-PVDF films on a cloudy day; (e) Corresponding sub-ambient temperature drops (ΔT); (f) Solar irradiance and ambient relative humidity; (g) Photograph, (h) thermal infrared photograph and (i) temperature tracking of model roofs covered with HP-PVDF film, AP-PVDF film, HAP-PVDF film and uncovered (from left to right) under direct sunlight.

https://doi.org/10.1007/s10118-024-3128-2

min test duration, noticeable temperature differences gradually emerged on all four roofs (Fig. S9 in ESI). These results illustrate that the HAP-PVDF film can be easily prepared over large areas without requiring sophisticated equipment, as it is atmospherically dried, thereby making it suitable for practical implementation in building thermal management.

CONCLUSIONS

In summary, we developed a hierarchical aligned porous structure for a PVDF film through freeze-thaw-promoted nonsolvent-induced phase separation, which demonstrates outstanding sub-ambient radiative cooling properties. This HAP-PVDF film possesses a unique combination of nano-, micro-, and oriented pores, along with the inherent high emission located within the atmospheric window. As a result, the HAP-PVDF film exhibits remarkable solar reflectance (~97%), high emissivity (~96%), and low thermal conductivity (0.038 $W \cdot m^{-1} \cdot K^{-1}$). Consequently, the HAP-PVDF film demonstrates excellent performance in daytime radiative cooling under direct sunlight conditions or in cloudy and humid conditions, achieving an average temperature reduction of 7 °C and a theoretical daytime cooling power of up to 94.8 $W \cdot m^{-2}$. Furthermore, the HAP-PVDF film demonstrates excellent flexibility and self-cleaning abilities, making them well-suited for outdoor applications. This study thus introduces a novel approach for the large-scale production of high-performance graded porous radiative cooling materials.

Conflict of Interests

The authors declare no interest conflict.

Electronic Supplementary Information

Electronic supplementary information (ESI) is available free of charge in the online version of this article at http://doi.org/10.1007/s10118-024-3128-2.

Data Availability Statement

The data that support the findings of this study are available from the corresponding author upon reasonable request. The authors' contact information: czhang@dhu.edu.cn (C.Z.) or txliu@jiangnan.edu.cn (T.X.L.).

ACKNOWLEDGMENTS

This work was financially supported by the National Natural Science Foundation of China (No. 52273067), the Fundamental Research Funds for the Central Universities (No. 2232023A-03), the Shuguang Program of Shanghai Education Development Foundation and Shanghai Municipal Education Commission (No. 23SG29).

REFERENCES

1 Abbasi, K. R.; Shahbaz, M.; Zhang, J.; Irfan, M.; Alvarado, R. Analyze the environmental sustainability factors of china: the role of fossil fuel energy and renewable energy. *Renew. Energy* **2022**, *187*, 390–402.
2 Aqilah, N.; Zaki, S. A.; Hagishima, A.; Rijal, H. B.; Yakub, F. Analysis on electricity use and indoor thermal environment for typical air-conditioning residential buildings in malaysia. *Urban Clim.* **2021**, *37*, 100830.
3 Maqbool, M.; Aftab, W.; Bashir, A.; Usman, A.; Guo, H.; Bai, S. Engineering of polymer-based materials for thermal management solutions. *Compos. Commun.* **2022**, *29*, 101048.
4 Xue, X.; Qiu, M.; Li, Y.; Zhang, Q. M.; Li, S.; Yang, Z.; Feng, C.; Zhang, W.; Dai, J. G.; Lei, D. Creating an eco-friendly building coating with smart subambient radiative cooling. *Adv. Mater.* **2020**, *32*, 1906751.
5 Raman, A. P.; Anoma, M. A.; Zhu, L.; Rephaeli, E.; Fan, S. Passive radiative cooling below ambient air temperature under direct sunlight. *Nature* **2014**, *515*, 540–544.
6 Zeng, S.; Pian,S.; Su, M.; Qing, Y.; Li, Xin.; Ma,Y.; Tao, G. Hierarchical-morphology metafabric for scalable passive daytime radiative cooling. *Science* **2021**, *373*, 692–696.
7 Tao, S.; Guan, F.; Chen, F.; Chen, M.; Fang, Z.; Lu, C.; Xu, Z. Construction of colorful super-omniphobic emitters for high-efficiency passive radiative cooling. *Compos. Commun.* **2021**, *28*, 100975.
8 Chan, K. Y.; Shen, X.; Yang, J.; Lin, K. T.; Venkatesan, H.; Kim, E.; Zhang, H.; Lee, J. H.; Yu, J.; Yang, J. Scalable anisotropic cooling aerogels by additive freeze-casting. *Nat. Commun.* **2022**, *13*, 5553.
9 Zhao, B.; Hu, M.; Ao, X.; Chen, N.; Pei, G. Radiative cooling: a review of fundamentals, materials, applications, and prospects. *Appl. Energy* **2019**, *236*, 489–513.
10 Chai, J.; Fan, J. Solar and thermal radiation-modulation materials for building applications. *Adv. Energy Mater.* **2022**, *13*, 2202932.
11 Xu, X.; Gu, J.; Zhao, H.; Zhang, X.; Dou, S.; Li, Y.; Zhao, J.; Zhan, Y.; Li, X. Passive and dynamic phase-change-based radiative cooling in outdoor weather. *ACS Appl. Mater. Interfaces* **2022**, *14*, 14313–14320.
12 Rephaeli, E.; Raman, A.; Fan, S. Ultrabroadband photonic structures to achieve high-performance daytime radiative cooling. *Nano Lett.* **2013**, *13*, 1457–1461.
13 Hossain, M. M.; Jia, B.; Gu, M. A metamaterial emitter for highly efficient radiative cooling. *Adv. Opt. Mater.* **2015**, *3*, 1047–1051.
14 Zhang, H.; Ly, K. C. S.; Liu, X.; Chen, Z.; Yan, M.; Wu, Z.; Wang, X.; Zheng, Y.; Zhou, H.; Fan, T. Biologically inspired flexible photonic films for efficient passive radiative cooling. *Proc. Natl. Acad. Sci.* **2020**, *117*, 14657–14666.
15 Yao, Z.; Yaoguang, M.; N., D. S.; Dongliang, Z.; Runnan, L.; Xiaobo, Y. Scalable-manufactured randomized glass-polymer hybrid metamaterial for daytime radiative cooling. *Science* **2017**, *355*, 1062–1066.
16 Li, X.; Peoples, J.; Yao, P.; Ruan, X. Ultrawhite $BaSO_4$ paints and films for remarkable daytime subambient radiative cooling. *ACS Appl. Mater. Interfaces* **2021**, *13*, 21733–21739.
17 Xiang, B.; Zhang, R.; Luo, Y.; Zhang, S.; Xu, L.; Min, H.; Tang, S.; Meng, X. 3D porous polymer film with designed pore architecture and auto-deposited SiO_2 for highly efficient passive radiative cooling. *Nano Energy* **2021**, *81*, 105600.
18 Sun, Y.; Ji, Y.; Javed, M.; Li, X.; Fan, Z.; Wang, Y.; Cai, Z.; Xu, B. Preparation of passive daytime cooling fabric with the synergistic effect of radiative cooling and evaporative cooling. *Adv. Mater. Technol.* **2021**, *7*, 2100803.
19 Zhou, K.; Li, W.; Patel, B. B.; Tao, R.; Chang, Y.; Fan, S.; Diao, Y.; Cai, L. Three-dimensional printable nanoporous polymer matrix composites for daytime radiative cooling. *Nano Lett.* **2021**, *21*, 1493–1499.

20 Jyotirmoy, M.; Yanke, F.; C., O. A.; Mingxin, J.; Kerui, S.; N., S. N.; Zhou, Z. H.; Xianghui, X.; Nanfang, Y.; Yuan, Y. Hierarchically porous polymer coatings for highly efficient passive daytime radiative cooling. *Science* **2018**, *362*, 315–319.
21 Shan, X.; Liu, L.; Wu, Y.; Yuan, D.; Wang, J.; Zhang, C.; Wang, J. Aerogel-functionalized thermoplastic polyurethane as waterproof, breathable freestanding films and coatings for passive daytime radiative cooling. *Adv. Sci.* **2022**, *9*, 2201190.
22 Zhong, H.; Li, Y.; Zhang, P.; Gao, S.; Liu, B.; Wang, Y.; Meng, T.; Zhou, Y.; Hou, H.; Xue, C. Hierarchically hollow microfibers as a scalable and effective thermal insulating cooler for buildings. *ACS Nano* **2021**, *15*, 10076–10083.
23 Yang, P.; He, J.; Ju, Y.; Zhang, Q.; Wu, Y.; Xia, Z.; Chen, L.; Tang, S. Dual-mode integrated Janus films with highly efficient NaH_2PO_2-enhanced infrared radiative cooling and solar heating for year-round thermal management. *Adv. Sci.* **2023**, *10*, 2206176.
24 Han, C.; Zhang, H.; Chen, Q.; Li, T.; Kong, L.; Zhao, H.; He, L. A directional piezoelectric sensor based on anisotropic PVDF/MXene hybrid foam enabled by unidirectional freezing. *Chem. Eng. J.* **2022**, *450*, 138280.
25 Munirasu, S.; Banat, F.; Durrani, A. A.; Haija, M. A. Intrinsically superhydrophobic PVDF membrane by phase inversion for membrane distillation. *Desalination* **2017**, *417*, 77–86.
26 Back, J.; Brandstätter, R.; Spruck, M.; Koch, M.; Penner, S.; Rupprich, M. Parameter screening of PVDF/PVP multi-channel capillary membranes. *Polymers* **2019**, *11*, 463.
27 Oikonomou, E. K.; Karpati, S.; Gassara, S.; Deratani, A.; Beaume, F.; Lorain, O.; Tencé-Girault, S.; Norvez, S. Localization of antifouling surface additives in the pore structure of hollow fiber PVDF membranes. *J. Membr. Sci.* **2017**, *538*, 77–85.
28 Wu, L.; Sun, J.; Wang, Q. Poly(vinylidene fluoride)/polyethersulfone blend membranes: effects of solvent sort, polyethersulfone and polyvinylpyrrolidone concentration on their properties and morphology. *J. Membr. Sci.* **2006**, *285*, 290–298.
29 Liao, X. L.; Sun, D. X.; Cao, S.; Zhang, N.; Huang, T.; Lei, Y. Z.; Wang, Y. Freely switchable super-hydrophobicity and super-hydrophilicity of sponge-like poly(vinylidene fluoride) porous fibers for highly efficient oil/water separation. *J. Hazard. Mater.* **2021**, *416*.
30 Jinlei, L.; Xueyang, W.; Dong, L.; Ning, X.; Bin, Z.; Shanhui, F.; Jia, Z. A tandem radiative/evaporative cooler for weather-insensitive and high-performance daytime passive cooling. *Sci. Adv.* **2022**, *8*, eabq0411.
31 Xu, Y.; Fang, Y.; Tao, S.; Fang, Z.; Ni, Y.; Lu, C.; Xu, C.; Li, W.; Xu, Z. A transparent radiative cooling emitter with multi-band spectral regulation for building energy saving. *Compos. Commun.* **2023**, *43*, 101717.
32 Cai, C.; Wei, Z.; Ding, C.; Sun, B.; Chen, W.; Gerhard, C.; Nimerovsky, E.; Fu, Y.; Zhang, K. Dynamically tunable all-weather daytime cellulose aerogel radiative supercooler for energy-saving building. *Nano Lett.* **2022**, *22*, 4106–4114.
33 Wang, T.; Wu, Y.; Shi, L.; Hu, X.; Chen, M.; Wu, L. A structural polymer for highly efficient all-day passive radiative cooling. *Nat. Commun.* **2021**, *12*, 365.

https://doi.org/10.1007/s10118-024-3128-2